

# Critical balance in magnetohydrodynamic, rotating and stratified turbulence: towards a universal scaling conjecture

By Sergei V. Nazarenko<sup>1,3</sup> and Alexander A. Schekochihin<sup>2,3</sup>

<sup>1</sup>Mathematics Institute, University of Warwick, Coventry CV4 7AL, UK

<sup>2</sup>Rudolf Peierls Centre for Theoretical Physics, University of Oxford, Oxford OX1 3NP, UK

<sup>3</sup>Institut Henri Poincaré, Université Pierre et Marie Curie, 75231 Paris Cedex 5, France

(Received 22 April 2009; Published in *J. Fluid Mech.* **677**, 134 (2011))

It is proposed that critical balance — a scale-by-scale balance between the linear propagation and nonlinear interaction time scales — can be used as a universal scaling conjecture for determining the spectra of strong turbulence in anisotropic wave systems. Magnetohydrodynamic (MHD), rotating and stratified turbulence are considered under this assumption and, in particular, a novel and experimentally testable energy cascade scenario and a set of scalings of the spectra are proposed for low-Rossby-number rotating turbulence. It is argued that in neutral fluids, the critically balanced anisotropic cascade provides a natural path from strong anisotropy at large scales to isotropic Kolmogorov turbulence at very small scales. It is also argued that the  $k_{\perp}^{-2}$  spectra seen in recent numerical simulations of low-Rossby-number rotating turbulence may be analogous to the  $k_{\perp}^{-3/2}$  spectra of the numerical MHD turbulence in the sense that they could be explained by assuming that fluctuations are polarised (aligned) approximately as inertial waves (Alfvén waves for MHD).

## 1. Introduction

Ability to support both linear waves and nonlinear interactions is ubiquitous in natural systems. Wave turbulence is, therefore, a very generic situation in such systems when dissipation coefficients are small and energy injected at some system-specific scale has to be dissipated at much smaller scales (Zakharov *et al.* 1992). Theory of turbulence is concerned with the ways in which the energy is transferred from large (injection) to small (dissipation) scales and, consequently, with the structure of the fluctuations in the intervening scale range.

A common property of many such systems is the presence of some mean field that introduces a special direction. Examples are plasmas embedded in a mean magnetic field, rotating fluids and stably stratified fluids with a mean temperature or density gradient (in real systems usually in the direction of gravity). Both linear and nonlinear physics is affected by the mean field: turbulent fluctuations in such systems tend to display a high degree of anisotropy. The typical wave numbers parallel and perpendicular to the special direction associated with the mean field often satisfy  $k_{\parallel} \ll k_{\perp}$ , while the wave dispersion relation is of the form

$$\omega = k_{\parallel} v(k_{\perp}). \quad (1.1)$$

For Alfvén waves in magnetohydrodynamics (MHD),  $v = v_A$ , the Alfvén speed, for inertial waves in rotating fluids,  $v = 2\Omega/k_{\perp}$ , where  $\Omega$  is the rotation frequency. Our

arguments will apply directly to these two cases; in stratified turbulence,  $k_{\parallel} \gg k_{\perp}$ , so the roles of  $k_{\parallel}$  and  $k_{\perp}$  are reversed and certain adjustments to the general argument will be needed — they are explained in section 5. Note that low-frequency waves in magnetised plasmas generally satisfy the gyrokinetic dispersion relation, which is also of the form (1.1) (Howes *et al.* 2006) and of which the Alfvén-wave dispersion relation is a large-scale limiting case.

The dispersion relation of the type (1.1) implies that waves propagate primarily in the parallel direction: indeed, the parallel and perpendicular group velocities are  $v_{\parallel} = v(k_{\perp})$  and  $v_{\perp} = (k_{\parallel}/k_{\perp})k_{\perp}v'(k_{\perp}) \ll v_{\parallel}$ . If the nonlinearity is of the fluid type,  $\mathbf{u} \cdot \nabla \mathbf{u}$ , where  $\mathbf{u}$  is the fluid velocity, then  $k_{\parallel} \ll k_{\perp}$  implies that nonlinear interactions are primarily perpendicular:  $\mathbf{u} \cdot \nabla \mathbf{u} \simeq \mathbf{u}_{\perp} \cdot \nabla_{\perp} \mathbf{u}$ , so the nonlinear decorrelation time is given by

$$\tau_{\text{NL}}^{-1} \sim k_{\perp} u_{\perp}(k_{\perp}), \quad (1.2)$$

where  $u_{\perp}(k_{\perp})$  is the characteristic velocity fluctuation amplitude corresponding to the wave number  $k_{\perp}$  (this formula assumes that fluctuations are not polarised in any particular way that might reduce the nonlinear interactions; if one assumes they are, in fact, so polarised, the scaling theory presented below has to be modified as explained in section 4.5). Note that incompressibility  $\nabla \cdot \mathbf{u} = 0$  and  $k_{\parallel} \ll k_{\perp}$  imply that the perpendicular motions are individually incompressible,  $\nabla_{\perp} \cdot \mathbf{u}_{\perp} = 0$  (see appendix A).

For anisotropic wave systems, Kolmogorov-style dimensional theory alone does not fix the scalings of the energy spectra. Indeed, assuming a local (in scale) energy cascade and hence a scale-independent energy flux  $\varepsilon$ ,

$$k_{\perp} E(k_{\perp}) \sim u_{\perp}^2(k_{\perp}) \sim \varepsilon \tau(k_{\perp}), \quad (1.3)$$

where  $E(k_{\perp})$  is the one-dimensional perpendicular energy spectrum and  $\tau(k_{\perp})$  is the “cascade time” corresponding to the characteristic wave number  $k_{\perp}$ . In the absence of waves or anisotropy, it is dimensionally inevitable that  $\tau(k) \sim \tau_{\text{NL}}(k)$ , whence  $E(k_{\perp}) \sim \varepsilon^{2/3} k_{\perp}^{-5/3}$ , the Kolmogorov spectrum. However, with waves and anisotropy, two additional dimensionless ratios arise:  $k_{\parallel}/k_{\perp}$  and  $\omega \tau_{\text{NL}} \sim k_{\parallel} v / k_{\perp} u_{\perp}$ , which measure the strength of the anisotropy and the relative time scales of the linear propagation and nonlinear interaction (equivalently, the relative size of the fluid velocity and the wave phase speed). The spectrum can, as far as dimensional theory is concerned, be an arbitrary function of these two ratios, both of which can have some nontrivial scaling with  $k_{\perp}$ .

Clearly, an additional physical assumption is necessary to fix the scalings. In strong MHD turbulence, it is known as the *critical balance (CB)* and states that the characteristic linear and nonlinear times are approximately equal at all scales:  $\omega \sim \tau_{\text{NL}}^{-1}$  (Higdon 1984; Goldreich & Sridhar 1995). We propose that CB be adopted more generally as a universal scaling conjecture for anisotropic wave turbulence. This removes the dimensional ambiguity in determining the cascade time, so we may set  $\tau \sim \tau_{\text{NL}}$  and recover the Kolmogorov spectrum,

$$E(k_{\perp}) \sim \varepsilon^{2/3} k_{\perp}^{-5/3}. \quad (1.4)$$

The CB itself,  $\omega \sim \tau_{\text{NL}}^{-1}$ , then gives us a relationship between the parallel and perpendicular scales:

$$k_{\parallel} \sim [\tau_{\text{NL}}(k_{\perp}) v(k_{\perp})]^{-1} \sim \varepsilon^{1/3} [v(k_{\perp})]^{-1} k_{\perp}^{2/3}. \quad (1.5)$$

Note that while these scaling arguments suggest that in some appropriately defined sense the energy distribution in the  $(k_{\perp}, k_{\parallel})$  plane will have a peak along the CB curve (1.5), they do not tell us what the functional shape of this distribution is (the “width” of the peak). However, as we will see in section 4.2, equation (1.5) is in fact sufficient to produce a testable quantitative prediction of the energy spectrum with  $k_{\parallel}$ .

In what follows, we first give a general argument in favour of the idea of CB (section 2) and then discuss three examples: MHD (and, more generally, plasma) turbulence, from whence these ideas originate (section 3), rotating turbulence, for which we propose a novel energy cascade scenario (section 4), and stratified turbulence (section 5). Note that in section 4.5, we propose the extension to the rotating turbulence of the concept of *polarisation alignment* (also originating from MHD turbulence; see Boldyrev 2006), which may help interpret the  $k_{\perp}^{-2}$  spectra reported in numerical simulations (Mininni *et al.* 2009; Thiele & Müller 2009). The section on rotating turbulence is the main part of this paper, while the MHD and stratified cases are discussed only briefly to emphasise what appears to be universal nature of some of the scaling arguments involved. In section 3.1 and in our concluding remarks (section 6), we will also mention a few other examples of CB emerging as a general physical principle in wave systems, including those that are different from the anisotropic wave type discussed here.

## 2. Why anisotropic turbulence is neither weak nor two-dimensional

In turbulent wave systems, if the fluctuation amplitudes at the injection scale are so small that  $\omega\tau_{\text{NL}} \gg 1$ , the nonlinearity can be treated perturbatively and what is known as weak turbulence theory emerges as a controlled approximation (Zakharov *et al.* 1992). In anisotropic wave systems, it typically predicts a turbulent cascade primarily in  $k_{\perp}$  (because the nonlinearity is primarily perpendicular), at constant  $k_{\parallel}$  — either exactly (in MHD; see Galtier *et al.* 2000) or approximately (in rotating turbulence; see Galtier 2003). While the analytic calculations can be quite involved, the basic result can be recovered in a simple nonrigorous way. If  $\omega\tau_{\text{NL}} \gg 1$ , nonlinear interactions between wave packets result in small perturbations of the amplitudes  $\delta u_{\perp} \sim (\omega\tau_{\text{NL}})^{-1} u_{\perp}$ . These perturbations can be assumed to accumulate as a random walk and then the cascade time  $\tau$  is by definition the time that it takes the cumulative perturbation to become comparable to the amplitude itself:  $n^{1/2}\delta u_{\perp} \sim u_{\perp}$ , where  $n \sim \tau\omega$  is the number of interactions. This gives  $\tau \sim \omega\tau_{\text{NL}}^2$  and, using equations (1.1-1.3), we get the one-dimensional perpendicular energy spectrum

$$E(k_{\perp}) \sim (\varepsilon k_{\parallel})^{1/2} [v(k_{\parallel})]^{1/2} k_{\perp}^{-2}. \quad (2.1)$$

We stress that since we have *assumed* that there is no parallel cascade, the energy injection rate  $\varepsilon$  can be an arbitrary function of  $k_{\parallel}$ . Thus, in equation (2.1) and in all other subsequent developments pertaining to weak turbulence,  $k_{\parallel}$  is a *parameter* — it is the characteristic parallel wave number at which energy is injected. For simplicity, one may assume that the injection is isotropic and so  $k_{\parallel} \sim k_0$ , the energy-injection wave number that will appear in sections 3 and 4. Note that in other anisotropic wave systems there can be a cascade in the parallel direction. The weak turbulence spectra for some such systems (historically the first example of anisotropic wave spectra) were found by Kuznetsov (1972). The parallel energy transfer in weak rotating turbulence (ignored by us) is discussed in great detail by Bellet *et al.* (2006).

Using equations (2.1) and (1.1-1.3), it is easy to work out the condition under which the weak turbulence approximation is valid:  $\omega\tau_{\text{NL}} \sim k_{\parallel} v(k_{\perp}) \varepsilon^{-1/3} k_{\perp}^{-2/3} \gg 1$ . Unless  $v(k_{\perp})$  increases sufficiently fast with  $k_{\perp}$ , the nonlinearity becomes stronger with increasing  $k_{\perp}$  compared to the linear propagation and the weak turbulence condition is broken at  $k_{\perp}$  given by equation (1.5). Thus, the weak turbulence cascade drives itself into a critically balanced state (see Schekochihin & Nazarenko 2011 for a somewhat less conventional but conceptually perhaps more convincing argument to this effect).

The opposite limit is a pure two-dimensional (2D) state:  $k_{\parallel}$  is assumed so small that

$\omega\tau_{\text{NL}} \ll 1$  and wave propagation is neglected. As generically happens in 2D, the energy cascade should then be inverse, from larger to smaller  $k_{\perp}$ . As  $k_{\perp}$  decreases,  $\tau_{\text{NL}}$  becomes longer, so the 2D approximation,  $\omega\tau_{\text{NL}} \ll 1$ , is eventually broken and CB is reached, at which point the turbulence is again three-dimensional (3D). Thus, both from the weak-turbulence limit (small amplitudes) and the 2D limit, the turbulence naturally evolves towards a state of CB.

There exists another argument, which is independent of the assumption of inverse cascade and suggests that 2D motions are fundamentally unstable. Consider two perpendicular planes separated by some distance. The motions in each plane will decorrelate on the time scale  $\tau_{\text{NL}}$ . In the parallel direction, information is transmitted by waves, so perfect correlation between the two planes required for a pure 2D state can only be sustained if a wave can propagate between them in a time shorter than  $\tau_{\text{NL}}$ . Thus, for any given  $k_{\perp}$ , there will be some parallel distance,  $k_{\parallel}^{-1}$ , given by the CB relation (1.5), beyond which the motions will decorrelate and become 3D. Thus, an initially 2D perturbation will tend to a state of CB (this argument was suggested to us by S. C. Cowley, 2004). This process can be interpreted as an instability of the 2D motions with respect to Cherenkov-type emission of waves.

### 3. MHD (Alfvénic) turbulence

The ideas laid out above in a general form originate from considerations of MHD turbulence. In MHD, equation (1.1) describes Alfvén waves with  $v = v_A = B_0/\sqrt{4\pi\rho}$ , where  $B_0$  is the mean magnetic field and  $\rho$  the density of the conducting fluid. Small anisotropic fluctuations in such a turbulence are Alfvénic,  $u_{\perp} \sim \delta B_{\perp}/\sqrt{4\pi\rho}$ , where  $\delta B_{\perp}$  is the perpendicular perturbation of the magnetic field (mathematically this statement can be formalised in terms of the Reduced MHD equations; see the end of appendix A).

Both weak-turbulence (Galtier *et al.* 2000) and 2D (Montgomery & Turner 1981) theories for MHD turbulence have been proposed. By the general arguments given above, both will naturally evolve towards a CB state,  $k_{\parallel}v_A \sim k_{\perp}u_{\perp}$ , with a Kolmogorov spectrum (1.4) and a scale-dependent anisotropy given by equation (1.5):

$$k_{\parallel} \sim \varepsilon^{1/3} v_A^{-1} k_{\perp}^{2/3}. \quad (3.1)$$

Note that as  $k_{\perp}$  increases, the turbulence becomes more anisotropic ( $k_{\parallel}/k_{\perp}$  decreases).

If the turbulence is weak at the injection scale, its spectrum is expected to be [see equation (2.1)]

$$E(k_{\perp}) \sim (\varepsilon k_{\parallel} v_A)^{1/2} k_{\perp}^{-2} \quad (3.2)$$

and there is no cascade in  $k_{\parallel}$  (Galtier *et al.* 2000). From equation (3.2),  $u_{\text{rms}} \sim (\varepsilon v_A/k_0)^{1/4}$ , where  $k_0$  is the wave number of energy injection (assumed isotropic), so  $\varepsilon \sim M_A^4 v_A^3 k_0$ , where  $M_A = u_{\text{rms}}/v_A \ll 1$  is the Alfvénic Mach number. Then the wave number at which weak turbulence breaks down and the critically balanced cascade begins is, from equation (3.1),

$$k_{\perp c} \sim \varepsilon^{-1/2} (k_{\parallel} v_A)^{3/2} \sim k_0 M_A^{-2}. \quad (3.3)$$

The anisotropy of Alfvénic turbulence and even equation (3.1) appear to have been confirmed by numerical simulations (Cho & Vishniac 2000; Maron & Goldreich 2001) and solar wind measurements (Horbury *et al.* 2008; Podesta 2009; Wicks *et al.* 2010; Chen *et al.* 2011) — this will be discussed further in section 4.2. The weak turbulence spectral scaling (3.2) has also been checked numerically (Perez & Boldyrev 2008). The precise nature of the scaling of the energy spectrum in the CB regime remains somewhat

mysterious: while the solar wind measurements support  $k_{\perp}^{-5/3}$  (e.g., Bale *et al.* 2005; Horbury *et al.* 2008; Sahraoui *et al.* 2009; Wicks *et al.* 2010; Chen *et al.* 2011), numerical simulations give spectra much closer to  $k_{\perp}^{-3/2}$  (Maron & Goldreich 2001; Mason *et al.* 2008) — a modified critical balance argument proposed by Boldyrev (2006) to explain these results will be discussed in section 4.5, where we will show how it can be adapted to the case of rotating turbulence.

### 3.1. Plasma turbulence

Beyond the MHD approximation, the gyrokinetic dispersion relation for low-frequency waves in magnetised plasmas is also of the form (1.1) (Howes *et al.* 2006). The general idea of a critically balanced cascade can be extended to various types of gyrokinetic turbulence, e.g., for plasma turbulence below the ion Larmor scale (Cho & Lazarian 2004; Schekochihin *et al.* 2009). Further details can be found in Schekochihin *et al.* (2009) (Sec. 7); the important point to keep in mind is that generalising the argument proposed in the present paper to plasma systems requires correctly identifying the cascading quantity (not always kinetic energy) and the type of nonlinearity (not always  $\mathbf{u} \cdot \nabla \mathbf{u}$ ).

In the case of the turbulence of kinetic Alfvén waves (dispersive waves that replace the MHD Alfvén waves below the ion Larmor scale), the scaling predictions resulting from the application of the CB conjecture to their dispersion relation (also of the form (1.1)) have been confirmed numerically (Biskamp *et al.* 1999; Cho & Lazarian 2004, 2009); the sub-Larmor-scale spectra and structure functions measured in the solar wind also appear to be consistent with the CB prediction (Sahraoui *et al.* 2009; Chen *et al.* 2010). This is the first example of confirmed applicability of the CB conjecture beyond its original target of MHD turbulence.

## 4. Rotating turbulence

Are magnetic anisotropy and magnetised plasma waves a special case or can CB be adopted as a universal scaling conjecture? A key test of universality would be to find a critically balanced cascade in a purely hydrodynamic setting. We propose the following scenario for the rotating turbulence.

### 4.1. Critically balanced rotating turbulence and restoration of isotropy

The dispersion relation for inertial waves in a rotating incompressible fluid is  $\omega = 2\Omega k_{\parallel}/k$ . Suppose that the energy is injected isotropically at some characteristic wave number  $k_0$  and the Rossby number  $\text{Ro} = u_{\text{rms}}k_0/\Omega \ll 1$ , i.e., the amplitudes at the injection scale are so low that turbulence is weak. Then the energy cascade will proceed anisotropically: let us assume for maximum simplicity that the parallel cascade is negligible, i.e.,  $k_{\parallel}$  stays of the order of  $k_0$  while energy moves towards larger  $k_{\perp}$  (Galtier 2003). When  $k_{\perp} \gg k_{\parallel}$ , the dispersion relation takes the form (1.1) with  $v(k_{\perp}) = 2\Omega/k_{\perp}$ ; the weak turbulence spectrum is then given by equation (2.1) [analogous to equation (3.2)]:

$$E(k_{\perp}) \sim (\varepsilon k_0 \Omega)^{1/2} k_{\perp}^{-5/2}. \quad (4.1)$$

Note that this implies  $u_{\text{rms}} \sim (\varepsilon \Omega)^{1/4} k_0^{-1/2}$  and so  $\varepsilon \sim \text{Ro}^4 \Omega^3 k_0^{-2}$ . As  $k_{\perp}$  increases, the nonlinearity becomes stronger and CB is reached at a critical  $k_{\perp}$  that can be inferred from equation (1.5) by setting  $k_{\parallel} \sim k_0$  [analogous to equation (3.3)]:

$$k_{\perp c} \sim \varepsilon^{-1/5} (k_{\parallel} \Omega)^{3/5} \sim k_0 \text{Ro}^{-4/5}. \quad (4.2)$$

For  $k_{\perp} > k_{\perp c}$ , the turbulence is no longer weak, but it is still anisotropic and the cascade is critically balanced: the spectrum is given by equation (1.4), while equation

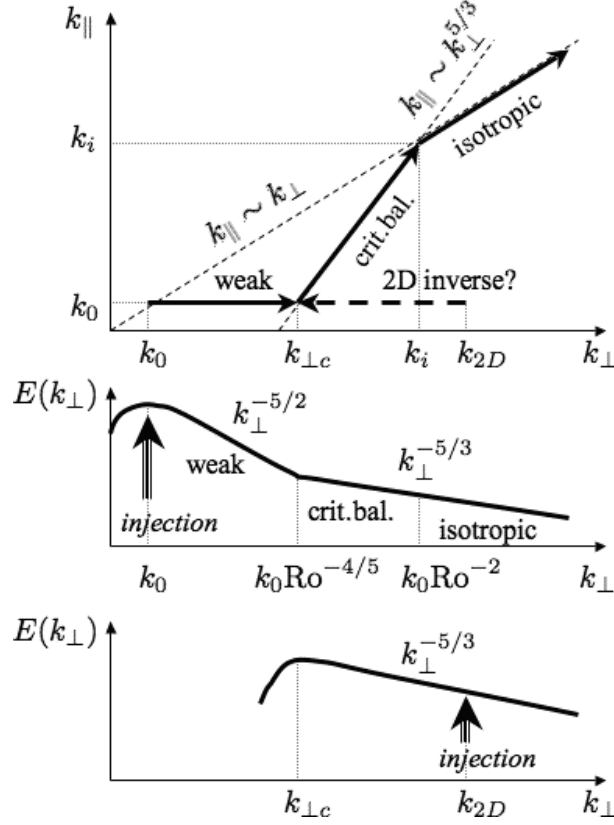


FIGURE 1. A sketch of cascade path and spectra for the rotating turbulence: both the case of injection at  $k_{\perp} = k_{\parallel} = k_0$  (and  $\text{Ro} \ll 1$ ) and that at  $k_{\parallel} \ll k_{\perp} = k_{2D}$  are shown (see sections 4.1 and 4.3). In the case of polarisation alignment, scalings shown in the two upper panels should be modified as explained in section 4.5. The absence of the parallel cascade in the weak regime is a simplifying assumption, as acknowledged at the start of section 4.1.

(1.5) becomes

$$k_{\parallel} \sim \varepsilon^{1/3} \Omega^{-1} k_{\perp}^{5/3} \quad (4.3)$$

(cf. Galtier *et al.* 2005). This relation is qualitatively different from the MHD case [equation (3.1)] in that the fluctuations become less, rather than more, anisotropic as  $k_{\perp}$  increases. Isotropy is reached when  $k_{\perp} \sim k_{\parallel} \sim k_i$ , where

$$k_i \sim \varepsilon^{-1/2} \Omega^{3/2} \sim k_0 \text{Ro}^{-2} \quad (4.4)$$

(cf. Zeman 1994). At this wave number, the velocity is  $u(k_i) \sim (\varepsilon/\Omega)^{1/2}$  (using equations (1.3) and (1.4)) and so the Rossby number at the corresponding scale is  $k_i u(k_i)/\Omega \sim 1$ . Therefore, at  $k > k_i$ , rotation is irrelevant and turbulence is of the familiar isotropic Kolmogorov type, with  $E(k) \sim \varepsilon^{2/3} k^{-5/3}$ . This is, of course, the physically inevitable outcome because unlike in the case of magnetised turbulence, which can feel the mean magnetic field at any scale, the hydrodynamic turbulence cannot feel the mean rotation rate if the local Rossby numbers are large. It is reassuring that the critically balanced cascade predicted by the general argument proposed here has naturally led to this Kolmogorov state.

The cascade path and the resulting spectrum are sketched in figure 1. We have illus-

trated the case discussed above, where energy is injected isotropically and in the weak turbulence regime. More generally, we expect that energy injected at a given  $(k_\perp, k_\parallel)$  will travel towards the CB path [equation (4.3)] followed by isotropic Kolmogorov cascade (as, e.g., shown in figure 1 for the case of quasi-2D injection, discussed in section 4.3). Obviously, if the energy is injected at  $k_0 > k_i$ , i.e., if  $Ro > 1$  at the injection scale, the cascade will start and remain isotropic because rotation can be ignored. Note that both the relationship (4.3) between the parallel and perpendicular scales and the wavenumber (4.4) of the transition to isotropy depend only on  $\varepsilon$  and  $\Omega$ , but not on the injection scale(s). Thus, the CB-to-isotropy path represents the “natural” state of rotating turbulence — probably applicable to the decaying case as well as the forced one. Thus, we suspect that equation (4.3) should prove to be a good prediction for the relationship between the parallel and perpendicular correlation lengths in the columnar vortical structures observed in experiments (e.g., Davidson *et al.* 2006).

Our predictions of the spectral slopes (4.1) and (1.4) and the scaling of the transition wave number (4.2) with  $Ro$  are experimentally and numerically verifiable (but see section 4.5 for possible alternative scalings). A transition from anisotropic to isotropic turbulence at the local  $Ro \sim 1$  [corresponding to the wave number  $k_i$ , equation (4.4)] appears to have been observed first by Jacquin *et al.* (1990). A change of spectral slope from  $\sim -2.2$  (perhaps consistent with  $-5/2$ ) to  $\sim -5/3$  [corresponding, in our theory, to the critical wave number  $k_{\perp c}$ , equation (4.2)] may have been observed in rotating turbulence experiments with small initial  $Ro$  (Fig. 5b in Morize *et al.* 2005), although it is premature to say if these results are definitely related to the transition to CB or merely to instrumental noise at high wave numbers. What does seem to be known definitely is that rotating turbulence has a clear tendency to a state where the local effective value of the Rossby number is  $\sim 1$ , i.e., the linear and nonlinear time scales are comparable and both linear and nonlinear dynamics are manifestly present (Davidson *et al.* 2006). This is consistent with the transition to CB that we are proposing and the nontrivial prediction is that whereas the spectrum is Kolmogorov for wave numbers above this transition  $k_\perp > k_{\perp c}$ , the turbulence remains anisotropic up to the second transition wave number  $k_i$ .

In designing or interpreting both laboratory and numerical experiments to test our predictions, one has to be mindful of the following caveat. In order for the full cascade path sketched in figure 1 to be realised, the system domain must be large enough to accommodate both the parallel and perpendicular scales implied by the CB state. If it is not, this will impose infrared cutoffs in the  $(k_\perp, k_\parallel)$  — these can restrict energy flows, possibly leading to 2D effects such as inverse cascades and (in periodic numerical simulations) finite-box effects such as formation of a  $k_\parallel = 0$  condensate (see further discussion in section 4.4).

Another important caveat concerns the absence (or negligibility) of the parallel cascade in the weak-turbulence regime. Unlike in the case of MHD turbulence, for rotating turbulence this is not an exact result, but an assumption (Galtier 2003) — and possibly a gross simplification of a fairly complicated precise situation (Bellet *et al.* 2006). We have made this simplification because the detailed properties of the weak-turbulence regime are less important in our view than its general tendency towards a strongly nonlinear CB state, in which the exact form of the resonant manifold in the wavenumber space is irrelevant.

#### 4.2. Local scale-dependent anisotropy

Quantitatively checking equation (4.3) is nontrivial. One possibility is to measure the energy spectrum with respect to parallel wave numbers: by definition,  $k_\parallel E(k_\parallel) \sim u_\perp^2 \sim$

$k_{\perp} E(k_{\perp})$ , so, using equations (1.4) and (4.3), we find a distinctive scaling:

$$E(k_{\parallel}) \sim \varepsilon^{4/5} \Omega^{-2/5} k_{\parallel}^{-7/5}, \quad k_0 < k_{\parallel} < k_i, \quad k_{\perp c} < k_{\perp} < k_i \quad (4.5)$$

(note that this is only valid in the CB regime). There is a similar result for Alfvén-wave turbulence based on equation (3.1):

$$E(k_{\parallel}) \sim \varepsilon v_A^{-1} k_{\parallel}^{-2}, \quad k_{\parallel} > k_0, \quad k_{\perp} > k_{\perp c} \quad (4.6)$$

which has recently been corroborated by the solar wind measurements (Horbury *et al.* 2008; Podesta 2009; Wicks *et al.* 2010; Chen *et al.* 2011).

It is from the MHD experience that one learns about an important subtlety in the definition of  $k_{\parallel}$  or, more precisely, of the parallel scale  $l_{\parallel} \sim k_{\parallel}^{-1}$  [in practice, scalings are usually extracted via structure functions rather than spectra:  $\delta u_{\perp}^2(l) \sim l^{-1} E(l^{-1})$ ]. In order for the scale-dependent anisotropy to become apparent,  $l_{\parallel}$  had to be defined with respect to the “local mean field,” i.e., the global mean magnetic field plus its perturbations at all scales larger than the one we are interested in (Cho & Vishniac 2000; Maron & Goldreich 2001; Horbury *et al.* 2008; Chen *et al.* 2011). Physically, this is because an Alfvénic perturbation can only “see” the local field, not the globally averaged one. Mathematically, measuring  $l_{\parallel}$  with respect to the global mean field would only capture the anisotropy of the largest-scale perturbation, while for all smaller-scale ones, such globally defined  $l_{\parallel}$  “slips off” one field line to a neighbouring one and effectively picks up perpendicular variation rather than the parallel one.

Similarly, for rotating turbulence, we anticipate that some scheme might have to be devised to measure parallel correlations along the local mean vorticity direction rather than along the global rotation axis. Indeed, it is physically intuitive that the inertial waves would propagate along the total vorticity  $\boldsymbol{\omega} = 2\boldsymbol{\Omega} + \delta\boldsymbol{\omega}$ , where  $\delta\boldsymbol{\omega} = \nabla \times \mathbf{u}$  (see further discussion in appendix A). In the CB regime, this deviation, while significant for measuring  $k_{\parallel}$ , is small:  $\delta\omega/\Omega \sim ku/\Omega \sim u/v \sim k_{\parallel}/k_{\perp} \ll 1$ ; once isotropy is restored,  $\delta\omega/\Omega \sim 1$  (so inertial waves no longer have a definite direction of propagation).

A practical method for measuring parallel correlations might be inspired by the wavelet (Horbury *et al.* 2008; Podesta 2009) or structure-function technique (Chen *et al.* 2010, 2011) used for the solar wind. Their method of measuring parallel spectra could in fact be taken as a good definition of what  $k_{\parallel}$  precisely means.

#### 4.3. Is inverse cascade possible in rotating turbulence?

Another interesting experimental possibility would be to stir the turbulence in a 2D way and find out whether it will develop an inverse cascade, bringing it first to the CB state and then to the isotropic Kolmogorov state. This possibility depends on the inverse cascade proceeding at a rate larger than the 2D structures radiating inertial waves, with energy thus directly transferred into the CB state (see the argument at the end of section 2 regarding the instability of a 2D state).

A putative inverse cascade followed by a direct critically balanced cascade is sketched in figure 1. Suppose the energy is injected at  $k_{\perp} = k_{2D} \gg k_{\parallel}$ . The inverse energy cascade, if it is sustainable, will give rise to the spectrum (1.4) for  $k_{\perp} < k_{2D}$ . This will extend, presumably at constant  $k_{\parallel}$ , to  $k_{\perp} \sim k_{\perp c}$ , given by the first expression in equation (4.2). At this point the turbulence is again 3D and the cascade should “turn around” and follow the CB path as before. Interestingly, the net perpendicular energy flux (integrated over  $k_{\parallel}$ ) is zero for  $k_{\perp} < k_{2D}$ , although the spectrum is  $k_{\perp}^{-5/3}$  extending to wave numbers both larger and smaller than  $k_{2D}$ , with the infrared cutoff given by  $k_{\perp c}$ . Since the velocity at  $k_{\perp c}$  is  $u_{\text{rms}} \sim \varepsilon^{2/5} (k_{\parallel} \Omega)^{-1/5}$ , we have  $k_{\perp c} \sim (k_{\parallel} \Omega / u_{\text{rms}})^{1/2}$ , where  $k_{\parallel}$  is the parallel wave



number at which the energy was injected. Note that the cascade reversal is a nontrivial consequence of anisotropy; in isotropic turbulence, zero flux would imply thermodynamic energy equipartition,  $E(k) \propto k^2$ .

Note that, as discussed at the end of section 4.1, a 2D inverse cascade can also occur in a geometrically constrained situation where the system domain restricts the cascade path and makes the turbulence effectively 2D: e.g., if the infrared cutoff in  $k_\perp$  lies to the right of the CB line in figure 1 (then the CB state cannot be reached and no cascade reversal is possible). Mathematically this means that the  $\partial/\partial z$  terms in equations (A 4) and (A 5) are negligible — without them, the perpendicular velocity decouples from the parallel one, the latter becomes a passive tracer and the former a 2D velocity field unaware of the rotation.

#### 4.4. Numerical evidence and finite-box effects

There is a large body of literature on numerical simulations of rotating turbulence. The two most recent and best resolved numerical studies are by Mininni *et al.* (2009) and Thiele & Müller (2009). We refer the reader to these papers for a comprehensive list of references to previous numerical work, which we will not replicate here. Let us discuss the results, which appear to be consistent in many independent investigations.

Relating numerical evidence to scaling theories like the one proposed above is far from straightforward because simulations are typically done in periodic boxes and we have not discussed the effects of finite dimensions of the containing volume on wave turbulence. For MHD turbulence, it was shown by Nazarenko (2007) that a finite box size along the mean magnetic field can lead to suppression of nonlinear interactions between modes with different  $k_\parallel$ . This results in a qualitatively different evolution of the 2D non-propagating  $k_\parallel = 0$  mode and the wave modes with finite  $k_\parallel$  (see also Bourouiba 2008; Boldyrev & Perez 2009; Schekochihin & Nazarenko 2011). Similar effects are probably operative in the numerical simulations of rotating turbulence, especially in relatively shallow boxes (because of the anisotropy, even cubic boxes are effectively shallow — this is well known in MHD turbulence, where simulations are routinely done in long boxes; see, e.g., Maron & Goldreich 2001; Mason *et al.* 2008). Both Mininni *et al.* (2009) and Thiele & Müller (2009) (as well as many previous publications, e.g., Smith & Waleffe 1999) report significant accumulation of energy in the  $k_\parallel = 0$  modes, via a nonlocal inverse cascade. The  $k_\parallel = 0$  modes also have a different spectrum than the finite- $k_\parallel$  modes. Note that in the local inverse cascade scenario of section 4.3, we envisioned energy injection at very small, but finite  $k_\parallel$  and did not consider the dynamics of the exact  $k_\parallel = 0$  modes (whose existence is particular to numerical boxes).

Another feature of the numerical simulations where the Rossby numbers associated with the forcing scale are low (the case we are considering in this paper) is what appears to be a robust  $k_\perp^{-2}$  scaling of the energy spectrum (see papers cited above and references therein). Is this a contradiction with the scaling predictions of section 4.1? It must be stressed here that the appearance of the  $k_\perp^{-2}$  spectrum cannot be explained by theories that assume weak *isotropic* turbulence and infer a  $k^{-2}$  spectrum (Dubrulle & Veldettaro 1992; Zeman 1994; Zhou 1995; Canuto & Dubovikov 1997), because numerical evidence appears clear that the turbulence is not isotropic. A similar problem was encountered in interpreting numerical simulations of MHD turbulence, which consistently give  $E \sim k_\perp^{-3/2}$  (Maron & Goldreich 2001; Mason *et al.* 2008), rather than  $k_\perp^{-5/3}$  that followed from the scaling arguments of section 3. There again, the  $k^{-3/2}$  spectrum that MHD turbulence would have if it were weak and isotropic (Iroshnikov 1963; Kraichnan 1965) is not relevant because MHD turbulence in these simulations is provably anisotropic. To resolve this

problem, Boldyrev (2006) proposed a modification of the CB argument based on the idea that nonlinearity is weakened in a scale-dependent fashion if the fluctuating fields align in a certain way. It turns out that a similar modification can be constructed for rotating turbulence and yields a spectrum that agrees with numerical evidence.

#### 4.5. Polarisation alignment

The estimate (1.2) for the nonlinear decorrelation time was correct subject to assuming implicitly that fluctuations are not polarised in any particular way that might weaken the nonlinearity, i.e., that the direction of  $\mathbf{u}_\perp$  decorrelates over the same scale as its amplitude. Let us consider what happens if we suppose instead that a typical turbulent fluctuation is three-dimensionally anisotropic with characteristic wave numbers  $k_x \gg k_y \gg k_z \equiv k_\parallel$ , where  $x$  is the direction of maximum gradients remaining approximately the same throughout the fluctuation and  $z$  the direction of the propagation of the inertial waves. Then, since in a system with  $k_\parallel \gg k_\perp$  the perpendicular velocity is individually incompressible,  $\nabla_\perp \cdot \mathbf{u}_\perp = 0$ , we have  $u_x \sim (k_y/k_x)u_y \ll u_y$ . Note that if we took  $k_y = 0$ , we would simply have a monochromatic inertial wave, which, as it is easy to show, is an exact nonlinear solution (see appendix A). However, if a wave packet of such waves is introduced, there would be nonlinear interaction and we are now attempting to determine how much the inertial-wave-like polarisation of fluctuations can be preserved in a strongly turbulent nonlinear state.

To estimate the nonlinear decorrelation time, we now replace equation (1.2) with

$$\tau_{\text{NL}}^{-1} \sim k_y u_y \sim k_\perp u_\perp(k_\perp) \theta(k_\perp), \quad (4.7)$$

where  $k_\perp \sim k_x$ ,  $u_\perp \sim u_y$  and  $\theta \sim k_y/k_x \sim u_x/u_y \ll 1$  is the velocity angle responsible for weakening the nonlinearity ( $\theta = 0$  would correspond to an inertial wave). To determine this angle, we need a physical hypothesis about the degree to which the inertial-wave polarisation of the velocity field is preserved across a typical turbulent fluctuation. We argued in section 4.2 that, physically speaking, inertial waves should propagate along the local mean vorticity direction rather than the global rotation axis and so the direction of anisotropy is scale-dependent. Thus, all directions within a fluctuation are determined to within an angular uncertainty  $\delta\theta \sim \delta\omega_\perp/\Omega$  set by the local value of the perpendicular vorticity fluctuation. One might then postulate that  $\theta \sim \delta\theta$ , i.e., that there is a tendency to preserve the inertial-wave polarisation to the maximal possible degree (*polarisation alignment* conjecture). Then

$$\theta \sim \frac{\delta\omega_\perp}{\Omega} \sim \frac{k_x u_\parallel}{\Omega} \sim \frac{u_y}{v}, \quad (4.8)$$

where we have taken  $u_\parallel \sim u_y$  (as in an inertial wave) and used  $v \sim \Omega/k_x$ . Therefore, equation (4.7) becomes

$$\tau_{\text{NL}}^{-1} \sim k_\perp [u_\perp(k_\perp)]^2 [v(k_\perp)]^{-1}. \quad (4.9)$$

Note that if we use the CB conjecture,  $\tau_{\text{NL}}^{-1} \sim k_\parallel v$ , and the fact that  $\theta \sim k_x/k_y$  by definition, we find from equations (4.7) and (4.8) that  $\theta \sim k_\parallel/k_y \sim (k_\parallel/k_x)^{1/2}$ ,  $k_y \sim (k_\parallel k_x)^{1/2}$ , and equation (4.9) can be rewritten as  $\tau_{\text{NL}}^{-1} \sim (k_\perp k_\parallel)^{1/2} u_\perp(k_\perp)$ .

Combining equations (4.9) and (1.3) and using CB,  $\tau \sim \tau_{\text{NL}} \sim (k_\parallel v)^{-1}$ , we find

$$E(k_\perp) \sim [\varepsilon v(k_\perp)]^{1/2} k_\perp^{-3/2} \sim (\varepsilon \Omega)^{1/2} k_\perp^{-2}, \quad (4.10)$$

$$k_\parallel \sim \varepsilon^{1/2} [v(k_\perp)]^{-3/2} k_\perp^{1/2} \sim \varepsilon^{1/2} \Omega^{-3/2} k_\perp^2. \quad (4.11)$$

These formulae replace equations (1.4) and (4.3) for rotating turbulence with polarisation

alignment. Equation (4.11) implies that isotropy is again restored at the wave number  $k_i$  given by equation (4.4), while the transition wave number from weak to critically balanced turbulence is, instead of equation (4.2), determined by

$$k_{\perp c} \sim \varepsilon^{-1/4} k_{\parallel}^{1/2} \Omega^{3/4} \sim k_0 \text{Ro}^{-1}. \quad (4.12)$$

The sketch of the cascade path in figure 1 is still valid, but with the new scalings for the CB regime (so at  $k_{\perp} = k_{\perp c}$ , the spectral slope now changes from  $-5/2$  to  $-2$  and at  $k_{\perp} = k_i$ , from  $-2$  to  $-5/3$ ; for  $k_{\perp c} < k_{\perp} < k_i$ ,  $k_{\parallel} \propto k_{\perp}^2$ ). The parallel spectrum is derived as in section 4.2 and so equation (4.5) is replaced by

$$E(k_{\parallel}) \sim \varepsilon [v(k_{\perp})]^{-1} k_{\parallel}^{-2} \sim \varepsilon^{3/4} \Omega^{-1/4} k_{\parallel}^{-3/2}. \quad (4.13)$$

Interestingly, Dubrulle & Valdettaro (1992) argue that a transition from  $k^{-2}$  to  $k^{-5/3}$  scaling is observed in the spectrum of motions in the galactic disk and might be attributable to a transition from rotating to standard isotropic Kolmogorov turbulence (although in their theory, the rotating turbulence is isotropic and weak, so the origin of their  $k^{-2}$  scaling is different than that proposed here).

Finally, we stress that the possibility of polarisation alignment in rotating turbulence (or a similar effect in MHD turbulence, discussed in section 4.6) does not undermine CB as a universal scaling conjecture — what is revised in this version of CB turbulence is the assumption of two-dimensional isotropy in the perpendicular plane.

#### 4.6. Polarisation alignment in MHD turbulence

The argument presented above is more or less analogous to the argument proposed by Boldyrev (2006) for MHD turbulence: he conjectured polarisation alignment between the perpendicular velocity and magnetic field fluctuations, which amounts to assuming that an Alfvén-wave polarisation is approximately preserved. The scalings he derived can be read off from equations (4.10), (4.11) and (4.13) by setting  $v(k_{\perp}) = v_A$  instead of  $2\Omega/k_{\perp}$  (note that equation (4.6) remains unchanged). Numerical simulations have confirmed both these scalings and specifically the scale-dependent alignment between the fields (Mason *et al.* 2008; Boldyrev *et al.* 2009; see, however, Beresnyak 2011). It appears plausible that the  $k_{\perp}^{-2}$  spectra observed in simulations of forced rotating turbulence (Mininni *et al.* 2009; Thiele & Müller 2009) could be similarly explained by the polarisation alignment argument we have given here. However, a word of caution: most solar wind measurements of Alfvénic turbulence do not support the  $k_{\perp}^{-3/2}$  scaling and incline rather towards  $k_{\perp}^{-5/3}$  (Bale *et al.* 2005; Horbury *et al.* 2008; Sahraoui *et al.* 2009; Wicks *et al.* 2010; Chen *et al.* 2011). Thus, it remains unclear whether polarisation alignment occurs in nature as well as in numerical boxes.

We note in passing that polarisation alignment may also be responsible for the robust  $k_{\perp}^{-3/2}$  spectra reported in simulations of 2D MHD turbulence (Biskamp & Welter 1989; Biskamp & Schwarz 2001). There is no “parallel” Alfvénic propagation there, but assuming  $k_x \gg k_y$ ,  $u_x \ll u_y$ ,  $\delta B_x \ll \delta B_y$ , and  $u_y \sim \delta B_y / \sqrt{4\pi\rho}$  still leads to a reduction of nonlinearity by  $\theta \sim k_y/k_x$ . This angle can again be assumed to scale with the typical angular uncertainty at a given scale:  $\theta \sim \delta B_y / \delta B_{\text{rms}}$ , where  $\delta B_{\text{rms}}$  is the rms amplitude of the magnetic fluctuations (i.e., the field at the outer scale). The argument is then the same as outlined in this section, leading to  $E(k_{\perp}) \sim (\varepsilon v_A)^{1/2} k_{\perp}^{-3/2}$ , where  $v_A = \delta B_{\text{rms}} / \sqrt{4\pi\rho} \sim (\varepsilon/k_0)^{1/3}$ . The CB conjecture does not come in here because there is no parallel linear propagation. This argument highlights an aspect of MHD that is not analogous to the rotating case: a pure 2D state for the latter is simply 2D hydrodynamics, with no effect from the rotation (see the end of section 4.3), whereas for MHD, setting

$\partial/\partial z = 0$  in equations (A 7) and (A 8) leaves velocities and magnetic fields still nonlinearly coupled via the Lorentz force. As we argued at the end of section 2, however, a pure 2D state is not sustainable in a 3D world, so exact 2D MHD is an artificial situation.

## 5. Stratified turbulence

Another hydrodynamic example where a critically balanced cascade should emerge is the stably vertically stratified turbulence, anisotropic with  $k_{\parallel} \gg k_{\perp}$ , where  $k_{\parallel}$  and  $k_{\perp}$  are the vertical and horizontal wave numbers, respectively (see, e.g., Cambon 2001; Godeferd & Staquet 2003; Laval *et al.* 2003; Kaneda & Yoshida 2004). The dispersion relation for (incompressible) gravity waves is  $\omega = Nk_{\perp}/k \approx Nk_{\perp}/k_{\parallel}$ , where  $N$  is the Brunt–Väisälä frequency. Since the roles of  $k_{\parallel}$  and  $k_{\perp}$  are reversed compared to the MHD and rotating turbulence, the arguments presented above have to be modified.

First, the incompressibility  $\nabla \cdot \mathbf{u} = 0$  now implies  $u_{\parallel} \sim (k_{\perp}/k_{\parallel})u_{\perp} \ll u_{\perp}$  (since  $k_{\perp} \ll k_{\parallel}$ , it is no longer true that  $\nabla_{\perp} \cdot \mathbf{u}_{\perp} = 0$  as was the case for MHD and rotating turbulence). This implies that the nonlinear interaction time continues to be given by equation (1.2). If CB is assumed, the horizontal energy spectrum is, therefore, still Kolmogorov [equation (1.4)], while the relationship between the horizontal and vertical wave numbers is [analogous to equations (3.1) and (4.3)]

$$k_{\perp} \sim \varepsilon N^{-3} k_{\parallel}^3 = l_O^2 k_{\parallel}^3, \quad (5.1)$$

where  $l_O = \varepsilon^{1/2} N^{-3/2}$  is called the Ozmidov (1992) scale. Using equation (5.1), we can calculate the vertical energy spectrum corresponding to the horizontal spectrum (1.4) in a way analogous to the derivation of equation (4.5):

$$E(k_{\parallel}) \sim N^2 k_{\parallel}^{-3}, \quad (5.2)$$

a spectrum previously proposed on dimensional grounds by Dewan (1997) and by Billant & Chomaz (2001). This argument is basically a reformulation in the CB language of the scaling hypothesis put forward by Lindborg (2006), to whose paper we refer the reader for discussion and references on the atmospheric measurements and numerical simulations, which appear to be consistent with this theory (see also Kaneda & Yoshida 2004; Lindborg & Brethouwer 2007).

The situation here is similar to rotating turbulence in that the anisotropy gets weaker as  $k_{\parallel}$  increases. The cascade becomes isotropic at the Ozmidov scale,  $k_{\perp} \sim k_{\parallel} \sim l_O^{-1}$ , where the local Froude number is  $u_{\perp}/l_O N \sim 1$ . At smaller scales, the turbulence cannot feel the mean gradient and becomes isotropic. Then both horizontal and vertical spectra are Kolmogorov, so there should be a spectral break at the Ozmidov scale for the vertical spectrum [transition from (5.2)], but not the horizontal one, which is Kolmogorov already in the CB regime. The cascade path is similar to figure 1 with  $k_{\parallel}$  and  $k_{\perp}$  swapped and equation (5.1) used for the CB line.

Despite these similarities, it must be acknowledged that because of the inversion of roles between  $k_{\parallel}$  and  $k_{\perp}$ , the case of stratified turbulence is perhaps somewhat special compared to the rather close analogy between MHD, plasma and rotating systems. In the latter cases, we had a two-dimensionally incompressible perpendicular turbulence and linear wave propagation in the 1D parallel direction setting the correlations between distant perpendicular 2D planes. In the case of stratified turbulence, the linear propagation is in the 2D horizontal plane, while the 1D vertical direction enters via wave dispersion and the nonlinearity ( $\tau_{\text{NL}}^{-1} \sim k_{\perp} u_{\perp} \sim k_{\parallel} u_{\parallel}$ ). Interestingly, the vertical spectrum (5.2), unlike its analogs (4.5) and (4.6), is independent of  $\varepsilon$ . Such flux-independent spectra

emerge quite commonly as a result of the break down of weak turbulence in 1D systems (e.g., Newell & Zakharov 2008; for discussions of universal flux-independent spectra see Denissenko *et al.* 2007 and Cardy *et al.* 2008, p. 12). They are often associated with formation of singular structures (see appendix B), a phenomenon we do not expect to be a key player in MHD or rotating turbulence. Thus, the CB in stratified turbulence might not be the whole story and the matter deserves further study. One can also envision quite complicated regimes and multiple scale ranges emerging in systems that are both rotating and stratified, e.g., the Earth’s atmosphere.

## 6. Conclusion

We have proposed that the critical balance of linear and nonlinear time scales, originally introduced for Alfvénic turbulence (Higdon 1984; Goldreich & Sridhar 1995) and more recently, for other types of magnetised plasma turbulence (Cho & Lazarian 2004; Schekochihin *et al.* 2009), should be used as a universal scaling conjecture for anisotropic turbulence in natural systems capable of supporting linear waves. While there are some indications that this idea works for stratified turbulence (Lindborg 2006), it has not been tested in rotating turbulence, for which we have proposed a novel energy cascade scenario and a set of verifiable predictions.

In neutral fluids, the two examples we have considered — rotating and stratified turbulence — suggest that the critically balanced cascade provides a path from the strongly anisotropic fluctuations caused by the presence of an external field (mean rotation or gradient) to isotropic Kolmogorov turbulence inevitable at sufficiently small scales (cf. Davidson *et al.* 2006). In that way, neutral fluids are different from conducting fluids and plasmas, where the presence of a mean magnetic field is felt at all scales and the anisotropy only gets stronger at smaller scales.

We observe that one might draw parallels between the CB principle and the “generalised Phillips spectra” (Newell & Zakharov 2008) that are thought to emerge from the break down of weak turbulence in many wave systems, e.g., surface water waves (Phillips 1958, 1985; Newell & Zakharov 2008), Rossby waves (Rhines 1975), Kelvin waves in cryogenic turbulence (Vinen 2000) and Bose-Einstein condensates (Proment *et al.* 2009). We note, however that some of these examples do not quite fit the anisotropic 3D type considered here and the break down of weak turbulence there may be related to formation of singular structures: this is discussed in more detail in appendix B.

We acknowledge important discussions with P. Berloff, S. Cowley, P. Davidson, K. Julien, J. McWilliams, F. Moisy and A. Newell. We are also grateful to the numerous anonymous referees for raising a number of important issues, which led to significant expansion and improvement of the paper. This work was supported by STFC (A.A.S.) and the Leverhulme Trust Network for Magnetised Plasma Turbulence.

## Appendix A. Reduced equations

A remarkable simplification of the underlying dynamical equations for turbulent fluctuations can be achieved by systematically taking into account their anisotropy. Here again CB serves as a guiding principle, but this time as an ordering assumption: the expectation that the linear and nonlinear time scales would be comparable tells one how to order the fluctuation amplitudes with the expansion parameter  $\epsilon = k_{\parallel}/k_{\perp}$ . This leads to reduced systems of equations, which are often more transparent physically and require less computational power to simulate numerically. An additional advantage of simulating

reduced equations is that the transition to the asymptotic anisotropic regime is carried out analytically and so does not eat up resolution.

Three well known examples of such reduced systems are the Reduced MHD (RMHD) equations for the Alfvénic turbulence (reproduced in section A.2) Electron Reduced MHD (ERMHD) equations for the turbulence of kinetic Alfvén waves at sub-Larmor scales and Hall Reduced MHD (HRMHD) equations for Alfvénic turbulence in cold-ion plasmas (all three are derived under the CB ordering in Schekochihin *et al.* 2009; the RMHD has been known since Strauss 1976; equations mathematically similar to ERMHD have been used to describe whistler turbulence in plasmas by, e.g., Biskamp *et al.* 1999; HRMHD has been studied by many authors, e.g., Gómez *et al.* 2008). A kinetic reduced system that emerges from the same principles is gyrokinetics (Frieman & Chen 1982; Howes *et al.* 2006), a general description of magnetised plasma turbulence of which RMHD, ERMHD and HRMHD are particular limits. All of these equations have been successfully simulated numerically (Perez & Boldyrev 2008; Cho & Lazarian 2009; Gómez *et al.* 2008; Howes *et al.* 2008); and in the case of RMHD and ERMHD, the results have explicitly been shown to be asymptotically consistent with simulations of the unreduced equations.

Here we explain the procedure for deriving a reduced system on the example of rotating turbulence, showing again its very close resemblance to magnetised fluid systems and providing concrete justification for some of the assumptions made in the main text.

#### A.1. Reduced rotating hydrodynamics

Our starting point is the Navier-Stokes equation for an incompressible fluid of viscosity  $\nu$  and density  $\rho = 1$  rotating at the rate  $\boldsymbol{\Omega} = \Omega \hat{\mathbf{z}}$  ( $z$  is the rotation axis):

$$\frac{\partial \mathbf{u}}{\partial t} + \mathbf{u} \cdot \nabla \mathbf{u} + 2\boldsymbol{\Omega} \times \mathbf{u} = -\nabla p + \nu \nabla^2 \mathbf{u}, \quad (\text{A } 1)$$

where  $p$  is pressure determined by  $\nabla \cdot \mathbf{u} = 0$ . This equation supports inertial waves with frequency  $\omega = \pm 2\Omega k_{\parallel}/k$  and corresponding eigenfunctions  $\mathbf{u} = (\pm i k_z/k, 1, \mp i k_x/k) u_y$ , where  $\mathbf{k} = (k_x, 0, k_z)$  without loss of generality. Note that for an inertial wave, the perturbed vorticity is aligned with velocity,  $\delta \boldsymbol{\omega} = \mp k \mathbf{u}$ , and so a monochromatic inertial wave is an exact nonlinear solution of equation (A 1) (because  $\mathbf{u} \cdot \nabla \mathbf{u} = \delta \boldsymbol{\omega} \times \mathbf{u} + \nabla u^2/2$ ; the gradient part can be absorbed into pressure).

In the anisotropic regime (low Rossby numbers), equation (A 1) is expanded in a small parameter  $\epsilon = k_{\parallel}/k_{\perp}$ . Using the CB as an ordering prescription, we order the time scale of the fluctuations as  $\omega \sim \epsilon \Omega \sim \mathbf{u}_{\perp} \cdot \nabla_{\perp}$ . We also order  $u_{\parallel} \sim u_{\perp}$  guided by the relationship between them in an inertial wave.

To lowest order in  $\epsilon$ ,  $\nabla \cdot \mathbf{u} = \nabla_{\perp} \cdot \mathbf{u}_{\perp} = 0$ , so the perpendicular motions are individually incompressible and can be represented by a stream function:  $\mathbf{u}_{\perp} = \hat{\mathbf{z}} \times \nabla_{\perp} \Phi$ . In the next order, the incompressibility condition allows us to find the divergence of the second-order correction to  $\mathbf{u}_{\perp}$  (to be useful shortly):

$$\nabla \cdot \mathbf{u} = \nabla_{\perp} \cdot \mathbf{u}_{\perp}^{(2)} + \frac{\partial u_{\parallel}}{\partial z} = 0. \quad (\text{A } 2)$$

The perpendicular part of equation (A 1) is (keeping two lowest orders)

$$\frac{\partial \mathbf{u}_{\perp}}{\partial t} + \mathbf{u}_{\perp} \cdot \nabla_{\perp} \mathbf{u}_{\perp} - \nu \nabla_{\perp}^2 \mathbf{u}_{\perp} = -2\Omega \hat{\mathbf{z}} \times \mathbf{u}_{\perp} - \nabla_{\perp} p. \quad (\text{A } 3)$$

In the lowest order, the left-hand side disappears and so right-hand side must vanish too. This gives  $p = 2\Omega \Phi$ . Now taking the perpendicular curl ( $\nabla_{\perp} \times$ ) of equation (A 3), we get

$$\frac{\partial}{\partial t} \nabla_{\perp}^2 \Phi + \{\Phi, \nabla_{\perp}^2 \Phi\} = 2\Omega \frac{\partial u_{\parallel}}{\partial z} + \nu \nabla_{\perp}^4 \Phi, \quad (\text{A } 4)$$

where  $\{f, g\} = \hat{\mathbf{z}} \cdot (\nabla_{\perp} f \times \nabla_{\perp} g)$  and we have used equation (A 2) to express  $\nabla_{\perp} \times (2\Omega \hat{\mathbf{z}} \times \mathbf{u}_{\perp}^{(2)}) = 2\Omega \hat{\mathbf{z}} \nabla_{\perp} \cdot \mathbf{u}_{\perp}^{(2)}$ . Finally, taking the parallel part of equation (A 1) to lowest order and using  $p = 2\Omega\Phi$ , we get

$$\frac{\partial u_{\parallel}}{\partial t} + \{\Phi, u_{\parallel}\} = -2\Omega \frac{\partial \Phi}{\partial z} + \nu \nabla_{\perp}^2 u_{\parallel}. \quad (\text{A } 5)$$

Equations (A 4) and (A 5) are the desired reduced system, which we will refer to as Reduced Rotating Hydrodynamics (RRHD). Up to notational differences, they are equivalent to the reduced system of Julien *et al.* (1998) (derived under slightly differently formulated assumptions; see also Julien & Knobloch 2007 and references therein for a uniform mathematical discussion of RRHD and reduced models generally). Let us itemise some of the properties of these equations:

- (a) they support inertial waves with  $\omega = \pm 2\Omega k_{\parallel}/k_{\perp}$  and corresponding eigenfunctions  $u_{\parallel} = \pm k_{\perp} \Phi$  (so, the wave is circularly polarised: as it propagates along  $\hat{\mathbf{z}}$ , the velocity vector rotates in the plane perpendicular to  $\mathbf{k}_{\perp}$ ); inertial-wave packets with fixed  $k_{\perp}$  and arbitrary amplitude are exact nonlinear solutions;
- (b) the velocity is  $\mathbf{u} = \hat{\mathbf{z}} \times \nabla_{\perp} \Phi + \hat{\mathbf{z}} u_{\parallel}$  and the (perturbed) vorticity  $\delta\boldsymbol{\omega} = -\hat{\mathbf{z}} \times \nabla_{\perp} u_{\parallel} + \hat{\mathbf{z}} \nabla_{\perp}^2 \Phi$ ; therefore, the RRHD equations can be written (omitting viscosity)

$$\frac{\partial}{\partial t} \nabla_{\perp}^2 \Phi + \{\Phi, \nabla_{\perp}^2 \Phi\} = (\delta\boldsymbol{\omega} + 2\boldsymbol{\Omega}) \cdot \nabla u_{\parallel}, \quad \frac{\partial u_{\parallel}}{\partial t} = -(\delta\boldsymbol{\omega} + 2\boldsymbol{\Omega}) \cdot \nabla \Phi, \quad (\text{A } 6)$$

thus, besides the 2D self-advection of the perpendicular velocity, the basic physical process is propagation of inertial waves along the total vorticity lines (recall section 4.2);

- (c) the 3D nature of the turbulence is enforced via *linear* propagation terms (recall section 2); when they are present, the system conserves one invariant, kinetic energy  $\int d^3\mathbf{r} (|\nabla_{\perp} \Phi|^2 + u_{\parallel}^2)/2$  and should have a direct cascade; when  $\partial/\partial z = 0$ , there are three invariants: perpendicular kinetic energy  $\int d^3\mathbf{r} |\nabla_{\perp} \Phi|^2/2$  (inverse cascade; recall section 4.3), enstrophy  $\int d^3\mathbf{r} |\nabla_{\perp}^2 \Phi|^2/2$  (direct cascade), and parallel kinetic energy  $\int d^3\mathbf{r} u_{\parallel}^2/2$  (direct cascade of a passive quantity);

- (d) while the RRHD equations were derived under the CB ordering, they allow both the weak and the strong turbulence regimes and so can track the transition from the former to the latter (section 4.1); they also remain valid if polarisation alignment occurs (section 4.5) and so can be used to measure and study it.

- (e) when nondimensionalising the RRHD equations, one can rescale the parallel and perpendicular distances separately (subject to appropriate rescaling of the amplitudes), i.e., the aspect ratio of the “box” is formally infinite — this is because the anisotropy of the fluctuations was the basis for the asymptotic expansion that led to RRHD; note that the scaling arguments of section 4 imply that the anisotropy of rotating turbulence diminishes with scale, so equations (A 4) and (A 5) will produce solutions that, at sufficiently small scales, violate the ordering assumptions behind the equations — this should be manifested by the development of ever finer parallel structure (see section 4.2).

## A.2. Reduced magnetohydrodynamics

Finally, for comparison, let us give the RMHD equations for the Alfvénic turbulence (derived from MHD in exactly the same way as RRHD was from equation (A 1); see, e.g., Schekochihin *et al.* 2009, section 2)

$$\frac{\partial}{\partial t} \nabla_{\perp}^2 \Phi + \{\Phi, \nabla_{\perp}^2 \Phi\} = v_A \frac{\partial}{\partial z} \nabla_{\perp}^2 \Psi + \{\Psi, \nabla_{\perp}^2 \Psi\} = v_A \hat{\mathbf{b}} \cdot \nabla \nabla_{\perp}^2 \Psi, \quad (\text{A } 7)$$

$$\frac{\partial \Psi}{\partial t} = v_A \frac{\partial \Phi}{\partial z} + \{\Psi, \Phi\} = v_A \hat{\mathbf{b}} \cdot \nabla \Phi, \quad (\text{A } 8)$$

where  $\Phi$  and  $\Psi$  are the stream functions of the perpendicular velocity and magnetic fluctuations:  $\mathbf{u}_\perp = \hat{\mathbf{z}} \times \nabla_\perp \Phi$ ,  $\delta \mathbf{B}_\perp = \hat{\mathbf{z}} \times \nabla_\perp \Psi$  (unlike in the rotating case, the parallel velocity and magnetic field fluctuations decouple and are passive with respect to the perpendicular ones; see Schekochihin *et al.* 2009), and  $\hat{\mathbf{b}} = \hat{\mathbf{z}} + \delta \mathbf{B}_\perp / B_0$  is the direction of the total magnetic field (along which the Alfvén waves propagate; recall section 4.2).

The similarities with the equations for rotating turbulence are obvious, but there are also differences originating from the physical differences between the inertial and Alfvén waves: the latter are non-dispersive ( $\omega = \pm k_\parallel v_A$ ), the perpendicular velocity and magnetic field fluctuations are linearly polarised and the eigenfunctions  $\Phi = \pm \Psi$  represent exact nonlinear solutions for arbitrary-shaped wave packets (the Elsasser 1950 solutions). It is also worth pointing out that whereas the coupling of  $\Phi$  to  $u_\parallel$  (perpendicular to parallel velocity) in equation (A 4) is purely linear, the coupling of  $\Phi$  to  $\Psi$  (velocity to magnetic field) in equation (A 7) is both linear and nonlinear (via the Lorentz force).

## Appendix B. Critical balance and coherent structures

It might appear tempting to relate the CB principle to the emergence of coherent structures for the following two reasons. Firstly, some coherent structures arise due to wave breaking, e.g., in the system of water surface gravity waves or internal gravity waves, and such a wave breaking occurs precisely when the nonlinearity becomes of order of the linear contributions. Secondly, in some well known examples of coherent structures, such as solitons or shocks, the linear and the nonlinear terms are in balance.

First, consider the coherent structures that result from wave breaking. Such structures are typically singular, e.g., the wave profile has a derivative discontinuity. To be specific, consider the water-surface gravity waves, where the CB approach, i.e., scale-by-scale balance of the linear and the nonlinear time scales, gives the well-known Phillips (1958) spectrum. Its connection to singular wave breaking structures has been widely discussed since it was first suggested by Kadomtsev (1965) and later adopted by Phillips (1985) himself (his original 1958 paper does not mention wave breaking). However, there is an uncertainty related to the geometry and the dimensionality of the wave crests. Kuznetsov (2004) argued that the Phillips spectrum should correspond to wave crests with singularity at isolated points (cone-like shapes) whereas more realistic 1D crests would give a different spectral exponent. Furthermore, coherent structures of different strengths or sizes can coexist and the resulting spectrum can depend on their distribution (e.g., in his refinement of the original theory Phillips 1985 introduced a distribution function for the crest lengths per unit area of the water surface). Thus, there is no obvious universal link between the CB state and singular coherent structures of the wave-breaking type: there may be structures with spectra different from the CB prediction, but one can also imagine a CB state without any singular structures at all.

Now let us turn to the nonsingular coherent structures. The most basic of the relevant nonlinear models is the Korteweg–de Vries (KdV) equation,  $u_t + uu_x + \mu u_{xxx} = 0$ , where  $\mu$  is the dispersion coefficient. Does CB work for KdV turbulence? Naively, the idea might seem promising because, the KdV model predicts formation of solitons — coherent structures in which the nonlinear and the linear terms are balanced, in the spirit of CB. Balancing the nonlinearity and dispersion scale by scale (the second and the third terms in the KdV equation), we get  $E(k) \sim k^3$ . However, if the separations between the solitons are much greater than their widths, then for the scales intermediate between the soliton width and the inter-soliton separation, the spectrum is that of a set of delta-functions, so  $E(k) \sim \text{const}$ , which is very different from the CB prediction. This is because the interaction is nonlocal in scale, whereas CB assumes locality. Note



also, that this is a 1D dispersive system and the physical arguments in favour of CB in anisotropic wave-supporting environments presented in section 2 do not generalise to it.

In conclusion, there does not seem to be a universal link between the CB and coherent structures. In some systems there may be coherent structures but not CB because the latter assumes locality, which is not automatically guaranteed. Even if both coherent structures and a CB spectrum are present, the former need not be the cause of the latter as coherent structures might occupy a negligible volume. Finally, we reiterate that the physical argument for the formation of a CB state in MHD, which, as we showed above, may similarly be applied to the rotating turbulence, does not invoke either wave breaking or coherent structures but is rather based on local nonlinear energy transfer and anisotropic spatial decorrelation arguments (section 2). As discussed at the end of section 5, the case of stratified turbulence is more ambiguous because there a CB-based argument leads to a flux-independent vertical spectrum (5.2) reminiscent of the Philips-type spectra produced by wave breaking. Whether this is a useful hint about the nature of stratified turbulence is clearly an intriguing question for future investigation.

## REFERENCES

- BALE, S. D., KELLOGG, P. J., MOZER, F. S., HORBURY, T. S. & REME, H. 2005 Measurement of the electric fluctuation spectrum of magnetohydrodynamic turbulence. *Phys. Rev. Lett.* **94**, 215002.
- BELLET, F., GODEFERD, F. S., SCOTT, J. F. & CAMBON, C. 2006 Wave turbulence in rapidly rotating flows. *J. Fluid Mech.* **562**, 83–121.
- BERESNYAK, A. 2011 The spectral slope and Kolmogorov constant of MHD turbulence. *Phys. Rev. Lett.* **106**, 075001.
- BILLANT, P. & CHOMAZ, J.-M. 2001 Self-similarity of strongly stratified inviscid flows. *Phys. Fluids* **13**, 1645–1651.
- BISKAMP, D. & SCHWARZ, E. 2001 On two-dimensional magnetohydrodynamic turbulence. *Phys. Plasmas* **8**, 3282–3292.
- BISKAMP, D., SCHWARZ, E., ZEILER, A., CELANI, A. & DRAKE, J. F. 1999 Electron magnetohydrodynamic turbulence. *Phys. Plasmas* **6**, 751–758.
- BISKAMP, D. & WELTER, H. 1989 Dynamics of decaying two-dimensional magnetohydrodynamic turbulence. *Phys. Fluids B* **1**, 1964–1979.
- BOLDYREV, S. 2006 Spectrum of magnetohydrodynamic turbulence. *Phys. Rev. Lett.* **96**, 115002.
- BOLDYREV, S., MASON, J. & CATTANEO, F. 2009 Dynamic alignment and exact scaling laws in magnetohydrodynamic turbulence. *Astrophys J.* **699**, L39–L42.
- BOLDYREV, S. & PEREZ, J. C. 2009 Spectrum of weak magnetohydrodynamic turbulence. *Phys. Rev. Lett.* **103**, 225001.
- BOUROUBA, L. 2008 Discreteness and resolution effects in rapidly rotating turbulence. *Phys. Rev. E* **78**, 056309.
- CAMBON, C. 2001 Turbulence and vortex structures in rotating and stratified flows. *Eur. J. Mech. B* **20**, 489–510.
- CANUTO, V. M. & DUBOVIKOV, M. S. 1997 A dynamical model for turbulence. V. The effect of rotation. *Phys. Fluids* **9**, 2132–2140.
- CARDY, J. L., FALKOVICH, G. & GAWEDZKI, K. 2008 *Non-equilibrium statistical mechanics and turbulence*. Cambridge: Cambridge University Press.
- CHEN, C. H. K., HORBURY, T. S., SCHEKOCIHIN, A. A., WICKS, R. T., ALEXANDROVA, O. & MITCHELL, J. 2010 Anisotropy of solar wind turbulence between ion and electron Scales. *Phys. Rev. Lett.* **104**, 255002.
- CHEN, C. H. K., MALLET, A., YOUSEF, T. A., SCHEKOCIHIN, A. A. & HORBURY, T. S. 2011 Anisotropy of Alfvénic turbulence in the solar wind and numerical simulations. *Mon. Not. R. Astron. Soc.* in press (E-print arXiv:1009.0662).
- CHO, J. & LAZARIAN, A. 2004 The anisotropy of electron magnetohydrodynamic turbulence. *Astrophys J.* **615**, L41–L44.

- CHO, J. & LAZARIAN, A. 2009 Simulations of electron magnetohydrodynamic turbulence. *Astrophys J.* **701**, 236–252.
- CHO, J. & VISHNIAC, E. T. 2000 The anisotropy of magnetohydrodynamic Alfvénic turbulence. *Astrophys J.* **539**, 273–282.
- DAVIDSON, P. A., STAPLEHURST, P. J. & DALZIEL, S. B. 2006 On the evolution of eddies in a rapidly rotating system. *J. Fluid Mech.* **557**, 135–144.
- DENISSENKO, P., LUKASCHUK, S. & NAZARENKO, S. 2007 Gravity wave turbulence in a laboratory flume. *Phys. Rev. Lett.* **99**, 014501.
- DEWAN, E. 1997 Saturated-cascade similitude theory of gravity wave spectra. *J. Geophys. Res.* **102**, 29799–29818.
- DUBRULLE, B. & VALDETTARO, L. 1992 Consequences of rotation in energetics of accretion disks. *Astron. Astrophys.* **263**, 387–400.
- ELSASSER, W. M. 1950 The hydromagnetic equations. *Phys. Rev.* **79**, 183–183.
- FRIEMAN, E. A. & CHEN, L. 1982 Nonlinear gyrokinetic equations for low-frequency electromagnetic waves in general plasma equilibria. *Phys. Fluids* **25**, 502–508.
- GALTIER, S. 2003 Weak inertial-wave turbulence theory. *Phys. Rev. E* **68**, 015301.
- GALTIER, S., NAZARENKO, S. V., NEWELL, A. C. & POUQUET, A. 2000 A weak turbulence theory for incompressible magnetohydrodynamics. *J. Plasma Phys.* **63**, 447–488.
- GALTIER, S., POUQUET, A. & MANGENEY, A. 2005 On spectral scaling laws for incompressible anisotropic magnetohydrodynamic turbulence. *Phys. Plasmas* **12**, 092310.
- GODEFERD, F. S. & STAQUET, C. 2003 Statistical modelling and direct numerical simulations of decaying stably stratified turbulence. Part 2. Large-scale and small-scale anisotropy. *J. Fluid Mech.* **486**, 115–159.
- GOLDREICH, P. & SRIDHAR, S. 1995 Toward a theory of interstellar turbulence. 2: Strong Alfvénic turbulence. *Astrophys J.* **438**, 763–775.
- GÓMEZ, D. O., MAHAJAN, S. M. & DMITRUK, P. 2008 Hall magnetohydrodynamics in a strong magnetic field. *Phys. Plasmas* **15**, 102303.
- HIGDON, J. C. 1984 Density fluctuations in the interstellar medium: evidence for anisotropic magnetogasdynamic turbulence. I — Model and astrophysical sites. *Astrophys J.* **285**, 109–123.
- HORBURY, T. S., FORMAN, M. & OUGHTON, S. 2008 Anisotropic scaling of magnetohydrodynamic turbulence. *Phys. Rev. Lett.* **101**, 175005.
- HOWES, G. G., COWLEY, S. C., DORLAND, W., HAMMETT, G. W., QUATAERT, E. & SCHEKOCIHIN, A. A. 2006 Astrophysical gyrokinetics: basic equations and linear theory. *Astrophys J.* **651**, 590–614.
- HOWES, G. G., DORLAND, W., COWLEY, S. C., HAMMETT, G. W., QUATAERT, E., SCHEKOCIHIN, A. A. & TATSUNO, T. 2008 Kinetic simulations of magnetized turbulence in astrophysical plasmas. *Phys. Rev. Lett.* **100**, 065004.
- IROSHNIKOV, R. S. 1963 Turbulence of a conducting fluid in a strong magnetic field. *Astron. Zh.* **40**, 742.
- JACQUIN, L., LEUCHTER, O., CAMBON, C. & MATHIEU, J. 1990 Homogeneous turbulence in the presence of rotation. *J. Fluid Mech.* **220**, 1–52.
- JULIEN, K. & KNOBLOCH, E. 2007 Reduced models for fluid flows with strong constraints. *J. Math. Phys.* **48**, 065405.
- JULIEN, K., KNOBLOCH, E. & WERNE, J. 1998 A new class of equations for rotationally constrained flows. *Theoret. Comput. Fluid Dynamics* **11**, 251–261.
- KADOMTSEV, B. B. 1965 *Plasma turbulence*. New York: Academic Press.
- KANEDA, Y. & YOSHIDA, K. 2004 Small-scale anisotropy in stably stratified turbulence. *New J. Phys.* **6**, 34.
- KRAICHNAN, R. H. 1965 Inertial-range spectrum of hydromagnetic turbulence. *Phys. Fluids* **8**, 1385–1387.
- KUZNETSOV, E. A. 1972 Turbulence of ion sound in a plasma located in a magnetic field. *Sov. Phys. JETP* **35**, 310.
- KUZNETSOV, E. A. 2004 Turbulence spectra generated by singularities. *JETP Lett.* **80**, 83–89.
- LAVAL, J.-P., MCWILLIAMS, J. C. & DUBRULLE, B. 2003 Forced stratified turbulence: successive transitions with Reynolds number. *Phys. Rev. E* **68**, 036308.

- LINDBORG, E. 2006 The energy cascade in a strongly stratified fluid. *J. Fluid Mech.* **550**, 207–242.
- LINDBORG, E. & BRETHOUWER, G. 2007 Stratified turbulence forced in rotational and divergent modes. *J. Fluid Mech.* **586**, 83–108.
- MARON, J. & GOLDBREICH, P. 2001 Simulations of incompressible magnetohydrodynamic turbulence. *Astrophys J.* **554**, 1175–1196.
- MASON, J., CATTANEO, F. & BOLDYREV, S. 2008 Numerical measurements of the spectrum in magnetohydrodynamic turbulence. *Phys. Rev. E* **77**, 036403.
- MININNI, P. D., ALEXAKIS, A. & POUQUET, A. 2009 Scale interactions and scaling laws in rotating flows at moderate Rossby numbers and large Reynolds numbers. *Phys. Fluids* **21**, 015108.
- MONTGOMERY, D. & TURNER, L. 1981 Anisotropic magnetohydrodynamic turbulence in a strong external magnetic field. *Phys. Fluids* **24**, 825–831.
- MORIZE, C., MOISY, F. & RABAUD, M. 2005 Decaying grid-generated turbulence in a rotating tank. *Phys. Fluids* **17**, 095105.
- NAZARENKO, S. 2007 2D enslaving of MHD turbulence. *New J. Phys.* **9**, 307.
- NEWELL, A. C. & ZAKHAROV, V. E. 2008 The role of the generalized Phillips' spectrum in wave turbulence. *Phys. Lett. A* **372**, 4230–4233.
- OZMIDOV, R. V. 1992 Length scales and dimensionless numbers in a stratified ocean. *Oceanology* **32**, 259–262.
- PEREZ, J. C. & BOLDYREV, S. A. 2008 On weak and strong magnetohydrodynamic turbulence. *Astrophys J.* **672**, L61–L64.
- PHILLIPS, O. M. 1958 The equilibrium range in the spectrum of wind-generated waves. *J. Fluid Mech.* **4**, 426–434.
- PHILLIPS, O. M. 1985 Spectral and statistical properties of the equilibrium range in wind-generated gravity waves. *J. Fluid Mech.* **156**, 505–531.
- PODESTA, J. J. 2009 Dependence of solar-wind power spectra on the direction of the local mean magnetic field. *Astrophys J.* **698**, 986–999.
- PROMENT, D., NAZARENKO, S. & ONORATO, M. 2009 Quantum turbulence cascades in the Gross-Pitaevskii model. *Phys. Rev. A* **80**, 051603.
- RHINES, P. B. 1975 Waves and turbulence on a beta-plane. *J. Fluid Mech.* **69**, 417–443.
- SAHRAOUI, F., GOLDSTEIN, M. L., ROBERT, P. & KHOTYANTSEV, Y. V. 2009 Evidence of a cascade and dissipation of solar-wind turbulence at the electron gyroscale. *Phys. Rev. Lett.* **102**, 231102.
- SCHEKOCHIHIN, A. A., COWLEY, S. C., DORLAND, W., HAMMETT, G. W., HOWES, G. G., QUATAERT, E. & TATSUNO, T. 2009 Astrophysical gyrokinetics: kinetic and fluid turbulent cascades in magnetized weakly collisional plasmas. *Astrophys J. Suppl.* **182**, 310–377.
- SCHEKOCHIHIN, A. A. & NAZARENKO, S. V. 2011 Weak Alfvén-wave turbulence revisited. *In preparation*.
- SMITH, L. M. & WALEFFE, F. 1999 Transfer of energy to two-dimensional large scales in forced, rotating three-dimensional turbulence. *Phys. Fluids* **11**, 1608–1622.
- STRAUSS, H. R. 1976 Nonlinear, three-dimensional magnetohydrodynamics of noncircular tokamaks. *Phys. Fluids* **19**, 134–140.
- THIELE, M. & MÜLLER, W. 2009 Structure and decay of rotating homogeneous turbulence. *J. Fluid Mech.* **637**, 425–442.
- VINEN, W. F. 2000 Classical character of turbulence in a quantum liquid. *Phys. Rev. B* **61**, 1410–1420.
- WICKS, R. T., HORBURY, T. S., CHEN, C. H. K. & SCHEKOCHIHIN, A. A. 2010 Power and spectral index anisotropy of the entire inertial range of turbulence in the fast solar wind. *Mon. Not. R. Astron. Soc.* **407**, L31–L35.
- ZAKHAROV, V. E., L'VOV, V. S. & FALKOVICH, G. 1992 *Kolmogorov Spectra of Turbulence I: Wave turbulence*. Berlin: Springer.
- ZEMAN, O. 1994 A note on the spectra and decay of rotating homogeneous turbulence. *Phys. Fluids* **6**, 3221–3223.
- ZHOU, Y. 1995 A phenomenological treatment of rotating turbulence. *Phys. Fluids* **7**, 2092–2094.